DETECTION OF THIN HIGH CONTRAST DIELECTRICS FROM BOUNDARY MEASUREMENTS

DAVID M. AMBROSE, EESHA DAS GUPTA, SHARI MOSKOW, VALENTINA OZORNINA, AND GIDEON SIMPSON

Abstract. We develop an efficient inversion method for thin high contrast scatterers when the contrast is on the order of the reciprocal of the thickness of the scatterer. We extend prior theory for the Helmholtz equation to arbitrary bounded domains and multiple scatterers in two and three dimensions to obtain a fast forward solver with complexity of one dimension lower. The lower-dimensional approximation is then paired with optimization to form the basis for parameter inversion. We show numerical results for the forward and inverse problems in two dimensions and describe extensions to Maxwell.

1. Introduction

It is well known in inverse scattering theory that if one has apriori information about the structure of the medium, aysymptotic approximation can be a tool to invert for relevant unknown parameters and may provide a natural regularization. Here we extend the results of one of the authors and her collaborators from [8] in this sense. There, Moskow, Santosa, and Zhang studied the Helmholtz equation in free space in the case of a thin, high contrast dielectric scatterer. In the limit as the height of the scatterer vanishes, simultaneously as the contrast goes to infinity, a limiting system of integral equations of one lower dimension was found to be satisfied. In the present contribution, we extend this theory to general bounded domains and multiple scatterers in two and three space dimensions and apply the lower-dimensional asymptotic approximation as a method for inversion. We find that the asymptotic results are similar in this case since the Green's functions, although different, have the same singularity.

Two of the authors, Ambrose and Moskow, previously worked with thin high contrast scatterers in the time-harmonic Maxwell equations (first analyzed in [3]), proving under some hypotheses that the thin high contrast problem has a somewhat different limiting system than for the Helmoltz case [2]. Ambrose, Gopalakrishnan, Moskow, and Rome subsequently used this limiting system as the basis of a method for inversion [1]. The inverse method in [1] was a direct method done under the assumption that the plane of the scatterer is known. In the present work, we also develop and implement (for Helmholtz) a method for inversion to locate the scatterer, but we do not make such an assumption and instead use an optimization algorithm.

In the case of low contrast, one approximates the scattered field by a known background or incident field which is then used in an integral formulation to yield the well known Born approximation, see for example [6]. A restatement of the Born approximation could be that a limiting problem, in which there is zero contrast, is used for inversion. We thus provide the high contrast analogue, loosely stated, by analyzing the case of infinite contrast, and using this for inversion. We find that unlike for the Born approximation, this high contrast analogue is nonlinear in the scatterer and captures interaction between multiple scatterers. This is also the case for other high contrast asymptotic limits such as in [4], [5].

Date: March 29, 2019.

The paper is organized as follows. In Section 2, we present the problem formulation for Helmholtz and describe the regime in which the analysis here will hold. Next, in Section 3 we show the asymptotic results. In Section 4 we describe the limiting solution for multiple scatterers and restate the main theorem for that case. In Section 5 we describe the change of variables for an arbitrary slit and show numerical results for the forward approximations, while Section 6 contains our inversion experiments. Finally in Section 7 we remark on how this approach can potentially be extended to Maxwell's equations using the Lippmann-Schwinger-type formulation shown rigorously to hold in [7].

2. Problem formulation

Here we consider a scalar wave problem on a smooth bounded domain Ω in $\mathbb{R}^d$, for $d = 2, 3$, modeled by the Helmholtz equation in the presence of a thin high contrast scatterer. The Helmholtz equation is given by

$$\Delta u_h + k^2 n_h^2 u_h = 0 \quad \text{in} \quad \Omega, \tag{1}$$

with Neumann boundary conditions

$$\frac{\partial u_h}{\partial \nu} = g \quad \text{on} \quad \partial\Omega,$$

where the coefficient $n_h^2(x)$ models the squared index of refraction of a thin high contrast scatterer. We assume that $n_h^2 - 1$ has support on a thin object $S_h \subset \Omega$. For simplicity we assume that Ω contains the origin, and that

$$S_h = S_0 \times (-h/2, h/2)$$

for S_0 a domain containing the origin in $\mathbb{R}^{d-1}$. We separate out the variable in the transverse direction and write $x = (\overline{x}, x_d)$. We assume that the scatterer is thin and high contrast in the sense that

$$n_h^2(x) = \begin{cases} n_0(\overline{x})/h, & \text{for} \quad x \in S_h, \\ 1, & \text{otherwise}. \end{cases} \tag{2}$$

That is, the analysis here applies to the regime where the contrast of the thin scatterer is on the order of its thickness, as was studied in [8] for the free space case. We assume for simplicity that $n_0(\overline{x})$ is continuous, although piecewise continuous and bounded in $L^\infty(S_0)$ would suffice. Related to the problem (1) is the corresponding background problem

$$\Delta u_{\mathbf{i}} + k^2 u_{\mathbf{i}} = 0 \quad \text{in} \quad \Omega, \tag{3}$$

with Neumann boundary conditions

$$\frac{\partial u_{\mathbf{i}}}{\partial \nu} = g \quad \text{on} \quad \partial\Omega.$$

Note that this solution corresponds to the field in the case when no scatterer exists in Ω, and is our analog to the incident wave in the free space setting. We assume also here that for given $n_h^2(x)$ and fixed h, k^2 is not an eigenvalue for (1) nor for (3), that is, for both problems we have existence of a unique solution.

If the scatterer S_h were to have bounded contrast, it is well known that for small thickness h the field u_h would be close to the background field $u_{\mathbf{i}}$. However, in our high contrast regime, the field will instead be close to the solution of a crack problem. To see this, we use the background Green's function and integration by parts to first write a Lippmann-Schwinger form of (1),

$$u_h(x) = u_{\mathbf{i}}(x) + k^2 \int_\Omega G(x, x')(n_h^2(x') - 1) u_h(x') dx', \tag{4}$$

where the Green's function G satisfies

$$(\Delta_x + k^2)G(x,x') = \delta_{x'}, \qquad \frac{\partial G}{\partial \nu_x} = 0 \text{ on } \partial\Omega. \tag{5}$$

Using the high contrast model (2), we also set $x' = (\overline{x}', x_d)$, so that (4) becomes

$$u_h(x) = u_{\mathbf{i}}(x) + k^2 \int_{S_0} \int_{-h/2}^{h/2} G(x, (\overline{x}', x_d'))(\frac{n_0(\overline{x}')}{h} - 1)u_h(\overline{x}', x_d')dx_d' d\overline{x}'. \tag{6}$$

Setting $z = x_d/h$ and $z' = x_d'/h$ and changing variables in the integral, one easily derives the limiting integral equation for u_0 on S_0,

$$u_0(\overline{x}) = u_{\mathbf{i}}((\overline{x},0)) + k^2 \int_{S_0} G((\overline{x},0),(\overline{x}',0))n_0(\overline{x}')u_0(\overline{x}')d\overline{x}'. \tag{7}$$

Solving for u_0 is a $d-1$ dimensional problem, and therefore yields a computationally efficient approximation to u_h in all of Ω,

$$u_h(x) \approx u_{\mathbf{i}}(x) + k^2 \int_{S_0} \int_{-h/2}^{h/2} G(x, (\overline{x}', x_d')) \left(\frac{n_0(\overline{x}')}{h} - 1 \right) u_0(\overline{x}')dx_d' d\overline{x}', \tag{8}$$

or the simpler and more efficient

$$u_h(x) \approx u_{\mathbf{i}}(x) + k^2 \int_{S_0} G(x, (\overline{x}',0))n_0(\overline{x}')u_0(\overline{x}')d\overline{x}'. \tag{9}$$

3. Estimates and convergence

We begin by formally deriving the first terms in an asymptotic expansion with respect to the parameter h, and then show convergence results. Taking $z = x_d/h$ which is as in [8] but with different notation, we define $\tilde{u}_h(\overline{x}, z) = u_h(\overline{x}, x_d)$ and the scaled version of (6),

$$\tilde{u}_h(\overline{x}, z)) = u_{\mathbf{i}}(\overline{x}, hz) + k^2 \int_{S_0} \int_{-1/2}^{1/2} G((\overline{x}, hz), (\overline{x}', hz'))(n_0(\overline{x}') - h)\tilde{u}_h(\overline{x}', z')dz' d\overline{x}'. \tag{10}$$

We write the ansatz

$$\tilde{u}_h(\overline{x}, z) = u_0(\overline{x}) + hu_1(\overline{x}, z) + \dots$$

and expand

$$u_{\mathbf{i}}(\overline{x}, hz) = u_{\mathbf{i}}(\overline{x}, 0) + hz\frac{\partial u_{\mathbf{i}}}{\partial x_d}(\overline{x}, 0) + \dots$$

and plug these into (10). The $O(1)$ terms yield the equation (7) for u_0. To obtain the $O(h)$ term we also need to expand the term

$$v_h(\overline{x}, hz) := \int_{S_0} \int_{-1/2}^{1/2} G((\overline{x}, hz), (\overline{x}', hz'))n_0(\overline{x}')u_0(\overline{x}')dz' d\overline{x}', \tag{11}$$

which we write at least formally as

$$v_h(\overline{x}, hz) = v_0(\overline{x}) + hv_1(\overline{x}, z) + o(h),$$

where

$$v_0(\overline{x}) = \int_{S_0} G((\overline{x},0),(\overline{x}',0))n_0(\overline{x}')u_0(\overline{x}')d\overline{x}'. \tag{12}$$

If we then match like powers of h we find that

$$\text{(13)}\quad u_1(\overline{x},z) = z\frac{\partial u_{\mathbf{i}}}{\partial x_d}(\overline{x},0) - k^2\int_{S_0}\int_{-1/2}^{1/2} G((\overline{x},0),(\overline{x}',0))n_0(\overline{x}')u_1(\overline{x}',z')dz'd\overline{x}' + k^2\int_{S_0}\int_{-1/2}^{1/2} G((\overline{x},0),(\overline{x}',0))u_0(\overline{x}')dz'd\overline{x}' - k^2 v_1(\overline{x},z).$$

Let $S = S_0 \times (-1/2, 1/2)$ be the scaled scatterer and define the operator $T : C^0(S) \to C^0(S)$ by

$$\text{(14)}\qquad Tg(\overline{x},z) = \int_{S_0}\int_{-1/2}^{1/2} G((\overline{x},0),(\overline{x}',0))n_0(\overline{x}')g(\overline{x}',z')dz'd\overline{x}',$$

where we also abuse notation and use T to denote the same operator from $L^2(S)$ to $L^2(S)$. Indeed, T is bounded and compact in both cases, since the singularity in G is the same as that of the free space fundamental solution, and so even when restricted to the lower-dimensional S_0 the kernel is only weakly singular. A detailed proof of this for free space G can be found in [8]. We note that the range of T contains only functions which are constant in z, and we can simplify (13) to

$$\text{(15)}\qquad (I + k^2 T)u_1(\overline{x},z) = z\frac{\partial u_{\mathbf{i}}}{\partial x_d}(\overline{x},0) - k^2 v_1(\overline{x},z) + k^2\int_{S_0} G((\overline{x},0),(\overline{x}',0))u_0(\overline{x}')d\overline{x}'.$$

The following lemma gives us an explicit expression for v_1.

Lemma 3.1. *Assume k^2 is not an eigenvalue for the problems (7), (3) so that the solution u_0 exists and is unique and that n_0 is continuous on S_0. If v_h is defined by (11) and v_0 is defined by (12), then*

$$v_1(\overline{x},z) := \lim_{h\to 0}\frac{v_h - v_0}{h} = -\frac{1}{2}u_0(\overline{x})n_0(\overline{x})\left(z^2 + \frac{1}{4}\right),$$

pointwise for $(\overline{x},z)$ in the interior of S.

Proof. Let $\mathcal{G}$ be the free space fundamental solution for the Helmholtz equation. Note that when $d = 3$ we have the formula

$$\mathcal{G}(x,x') = \frac{\exp ik|x-x'|}{4\pi|x-x'|},$$

and when $d = 2$ we have instead

$$\mathcal{G}(x,x') = \frac{i}{4}H_0^{(1)}(k|x-x'|),$$

for $H_0^{(1)}$ the Hankel function of the first kind. Then the difference $G - \mathcal{G}$ satisfies a homogeneous Helmholtz equation in Ω with Neumann data equal to the normal derivative of $\mathcal{G}$, which will be smooth for x' bounded away from the boundary of Ω. For any smooth integrand ϕ, we have

$$\int_{S_0}\int_{-1/2}^{1/2}\phi((\overline{x},hz),(\overline{x}',hz'))dz'd\overline{x}' = \int_{S_0}\phi((\overline{x},0),(\overline{x}',0))d\overline{x}' + O(h^2),$$

by Taylor expansion and the fact that the linear term integrates to zero. Hence

$$\lim_{h\to 0}\frac{v_h - v_0}{h} = \lim_{h\to 0}\frac{1}{h}\int_{S_0}\int_{-1/2}^{1/2}\left(\mathcal{G}((\overline{x},hz),(\overline{x}',hz')) - \mathcal{G}((\overline{x},0),(\overline{x}',0))\right)n_0(\overline{x}')u_0(\overline{x}')dz'd\overline{x}',$$

and the result follows by Proposition 2 of [8]. We note that the explicit formula is obtained by integrating in a small cylinder around the singularity since we know $\mathcal{G}$ explicitly, and does not hold uniformly for $\overline{x}$ up to the boundary of S_0. ☐

Lemma 3.1 means that the equation (15) for u_1 becomes

$$(16)\quad (I+k^2T)u_1(\overline{x},z) = z\frac{\partial u_{\mathbf{i}}}{\partial x_d}(\overline{x},0) + \frac{k^2}{2}u_0(\overline{x})n_0(\overline{x})\left(z^2+\frac{1}{4}\right) + k^2\int_{S_0} G((\overline{x},0),(\overline{x}',0))u_0(\overline{x}')d\overline{x}'.$$

Since functions in the range of the operator T do not depend on the z variable, we see that if we write

$$(17)\qquad u_1(\overline{x},z) = \hat{u}_1(x) + z\frac{\partial u_{\mathbf{i}}}{\partial x_d}(\overline{x},0) + \frac{k^2}{2}z^2u_0(\overline{x})n_0(\overline{x})$$

this will indeed solve (16) if $\hat{u}_1$ is the solution to the lower-dimensional integral equation given by

$$(18)\quad (I+k^2T)\hat{u}_1(\overline{x}) = \frac{k^2}{8}u_0(\overline{x})n_0(\overline{x}) + k^2\int_{S_0} G((\overline{x},0),(\overline{x}',0))u_0(\overline{x}')d\overline{x}' - \frac{k^4}{24}\int_{S_0} G((\overline{x},0),(\overline{x}',0))u_0(\overline{x}')n_0^2(\overline{x})d\overline{x}'.$$

Proposition 3.2. *Assume k^2 is not an eigenvalue for (1), (3) so that (4) has a unique solution $u_h \in C^0(S_h)\cap H^2(\Omega)$. Assume also that $-1/k^2$ is not an eigenvalue for T given by (14), and let $u_0(x') \in C^0(S_0)$ be the unique solution to (7), extended to all of S_h by $u_0(x',x_d) := u_0(x')$. Then there exists $C>0$, independent of h, such that the following estimate holds:*

$$\|u_h - u_0\|_{C^0(S_h)} \le Ch.$$

Furthermore, if u_0 is extended to all of Ω by the right hand side of (9) we have that

$$\|u_h - u_0\|_{L^\infty(\Omega)} \le Ch.$$

Proof. The proof of the first result follows as in [8], but we give an abbreviated version for completeness. One sees that for T defined by (14),

$$(19)\quad (I+k^2T)(\tilde{u}_h - u_0) = u_{\mathbf{i}}((\overline{x},hz) - u_{\mathbf{i}}(\overline{x},0) + hk^2\int_{S_0}\int_{-1/2}^{1/2} G((\overline{x},hz),(\overline{x}',hz'))\tilde{u}_h(\overline{x}',z')dz'd\overline{x}' + k^2\int_{S_0}\int_{-1/2}^{1/2}\left(G((\overline{x},0),(\overline{x}',0)) - G((\overline{x},hz),(\overline{x}',hz'))\right)\tilde{u}_h(\overline{x}',z')n_0(\overline{x}')dz'dx'.$$

Lemma 1 of [8] says that for the free space fundamental solution

$$\sup_{(\overline{x},z)\in S}\int_{S_0} |\mathcal{G}((\overline{x},0),(\overline{x}',0)) - \mathcal{G}((\overline{x},hz),(\overline{x}',hz'))|d\overline{x}' \le Ch,$$

which implies the bound

$$(20)\qquad \sup_{(\overline{x},z)\in S}\int_{S_0} |G((\overline{x},0),(\overline{x}',0)) - G((\overline{x},hz),(\overline{x}',hz'))|d\overline{x}' \le Ch,$$

since $\mathcal{G}$ and G differ by a smooth function for $(\overline{x},z)\in S$. Using this and noting that the right-hand side of (19) is continuous, and we can bound the residual by

$$(21)\qquad \|(I+k^2T)(\tilde{u}_h - u_0)\|_{C^0(S)} \le h\|u_{\mathbf{i}}\|_{C^1(S)} + Ch\|\tilde{u}_h\|_{C^0(S)}$$

where we have combined the last two terms of (19). Using the triangle inequality yields

$$(22)\qquad \|(I+k^2T)(\tilde{u}_h - u_0)\|_{C^0(S)} \le h\|u_{\mathbf{i}}\|_{C^1(S)} + Ch\|\tilde{u}_h - u_0\|_{C^0(S)} + Ch\|u_0\|_{C^0(S)}.$$

By our assumption that $-1/k^2$ is not an eigenvalue of T, the Fredholm theory implies that $(I+k^2T)^{-1}$ is a bounded operator on $C^0(S)$. This, combined with moving the second term on the right-hand side of (22) over to the left-hand side yields the first result. For the second bound, first we abuse notation somewhat extend u_0 to be

$$u_0(x) = u_{\mathbf{i}}(x) + k^2 \int_{S_0} G(x, (\overline{x}', 0)) n_0(\overline{x}') u_0(\overline{x}') d\overline{x}', \tag{23}$$

where inside the integral u_0 refers to the $d-1$ dimensional solution to (7). We invoke (6) to write the difference as

$$\begin{aligned} &u_h(x) - u_0(x) \\ &= k^2 \int_{S_0} \int_{-1/2}^{1/2} \big(G(x, (\overline{x}', hz'))(n_0(\overline{x}') - h)\tilde{u}_h(\overline{x}', z') - G(x, (\overline{x}', 0)) n_0(\overline{x}') u_0(\overline{x}') \big) \, dz' d\overline{x}'. \end{aligned} \tag{24}$$

Note that (20) holds for any $x \in \Omega$, so the result follows from that and the the first estimate in this proposition. □

Proposition 3.3. *Assume k^2 is not an eigenvalue for (1), (3) so that (4) has a unique solution $u_h \in C^0(S_h) \cap H^2(\Omega)$. Assume also that $-1/k^2$ is not an eigenvalue for T given by (14). Let $u_0(x') \in C^0(S_0)$ be the unique solution to (7), extended to all of S_h by $u_0(x', x_d) := u_0(x')$, and let u_1 be defined by (17) where $\hat{u}_1$ is the unique solution to (18). Then we have that*

$$\|\tilde{u}_h - (u_0 + h u_1)\|_{L^2(S)} = o(h).$$

Proof. We again describe briefly the proof which is as in [8]. One again can calculate the residual

$$\begin{aligned} (I + k^2 T)(\tilde{u}_h - (u_0 + h u_1)) &= u_{\mathbf{i}} - \left(u_{\mathbf{i}}(\overline{x}, 0) + hz \frac{\partial u_{\mathbf{i}}}{\partial x_d}(\overline{x}, 0) \right) \\ &+ k^2 h \int_S G((\overline{x}, hz), (\overline{x}', hz')) \tilde{u}_h(\overline{x}', z') d\overline{x}' dz' - hk^2 \int_S G((\overline{x}, 0), (\overline{x}', 0)) u_0(\overline{x}') dx' \\ &+ k^2 (v_0(\overline{x}) - v_h(\overline{x}, hz)) - h \frac{k^2}{2} \left(z^2 + \frac{1}{4} \right) u_0(\overline{x}) n_0(\overline{x}) \\ &+ k^2 \int_S \big(G((\overline{x}, 0), (\overline{x}', 0)) - G((\overline{x}, hz), (\overline{x}', hz')) \big) \, n_0(\overline{x}')(\tilde{u}_h - u_0) d\overline{x}' dz'. \end{aligned} \tag{25}$$

There are seven terms on the right-hand side of (25), and of these, the first, second, third, fourth, and seventh are $O(h^2)$ in $L^2(S)$ because of the smoothness of $u_{\mathbf{i}}$, (20), and Proposition 3.2. We therefore focus on the fifth and sixth terms, which we will now group together as one quantity; this is pointwise $o(h)$ from Lemma 3.1. If we divide by h, it is pointwise almost everywhere going to zero, and by (20) uniformly bounded. The Lebesgue dominated convergence theorem implies therefore that it is going to zero in $L^2(S)$. Hence the right hand side of (25) is $o(h)$ in $L^2(S)$. Again by our assumption that $-1/k^2$ is not an eigenvalue of T and the Fredholm theory we have that $(I + k^2 T)^{-1}$ is a bounded operator on $L^2(S)$, and hence the result follows. □

4. Multiple scatterers

For the Born approximation and other fixed contrast asymptotic regimes, in the first order approximations the scatterers are decoupled from one another, and so multiple scattering effects can not be captured without higher-order corrections. Furthermore, in many cases the scatterers need to be well separated from one another for the approximations to be valid. In the high contrast regime studied here, the limiting problem both captures multiple scattering and is valid for close and even crossing thin scatterers. We consider $d = 2$ for simplicity in what follows, but similar results can be obtained when $d = 3$. Assume that n_h^2 takes the more general form

$$n_h^2(x) = \begin{cases} n_0^{(j)}(x)/h_j, & \text{for } \ x \in S_{h_j}^j, \\ 1, & \text{otherwise}, \end{cases} \tag{26}$$

where for $j = 1, \ldots, m$, we have a line segment S_0^j contained in Ω and for which the strip

$$S_{h_j}^j = \{x \pm h\nu_j |\ x \in S_0^j \text{ and } \ 0 \leq h < h_j\}$$

is also contained in Ω, where ν_j is the unit normal to the line segment S_0^j. We assume that the line segments S_0^j are not overlapping for segments of positive measure in one dimension, but we allow them to possibly intersect at points, assuming that n_h^2 is well-defined. We will let

$$S_h = \bigcup_j S_{h_j}^j \ \text{ and } \ S_0 = \bigcup_j S_0^j$$

be the set of strips and the finite set of limiting line segments respectively. We assume also that $n_0^{(j)}$ varies only in the direction tangential to S_0^j. Then as before we consider the solution to

$$\Delta u_h + k^2 n_h^2 u_h = 0 \ \text{ in } \ \Omega, \tag{27}$$

with n_h defined by (26) and with Neumann boundary conditions

$$\frac{\partial u_h}{\partial \nu} = g \ \text{ on } \ \partial\Omega.$$

Corresponding to this is the limiting problem to find $u_0 \in C^0(S_0)$ such that

$$u_0(x) = u_{\mathbf{i}}(x)|_{S_0} + \sum_{j=1}^m k^2 \int_{S_0^j} G(x, x')|_{S_0 \times S_0^j} n_0^{(j)}(x') u_0(x')|_{S_0^j} d\sigma_{x'}. \tag{28}$$

We define the operators $T_j : C^0(S_0) \to C^0(S_0)$ through the formula

$$T_j g(x) = \int_{S_0^j} G(x, x')|_{S_0 \times S_0^j} n_0^{(j)}(x') g(x')|_{S_0^j} d\sigma_{x'}, \tag{29}$$

and letting

$$T = \sum_{j=1}^m T_j,$$

the problem (28) becomes

$$(I + k^2 T) u_0 = u_{\mathbf{i}}(x)|_{S_0}.$$

By linear transformations one has the analogue of (20) on each $S_0^{(j)}$, and from the proof of (3.2) one has the following theorem:

Proposition 4.1. *Assume k^2 is not an eigenvalue for (27), (3) so that the Lippmann-Schwinger form of (27) has a unique solution $u_h \in C^0(S_h) \cap H^2(\Omega)$. Assume also that $-1/k^2$ is not an eigenvalue for $T = \sum_{j=1}^m T_j$, with each T_k given by (29), and let $u_0(x') \in C^0(S_0)$ be the unique solution to (28), extended to all of S_h by $u_0(x', x_d) := u_0(x')$. Let $h_{max} = \max_j h_j$. Then for some C independent of h_{max}, we have the bound*

$$\|u_h - u_0\|_{C^0(S_h)} \leq C h_{max}.$$

Furthermore, if u_0 is extended to all of Ω by

$$u_0(x) = u_{\mathbf{i}}(x) + \sum_{j=1}^m k^2 \int_{S_{h_j}^j} G(x, x') n_0^{(j)}(x')/h_j u_0(x') dx', \tag{30}$$

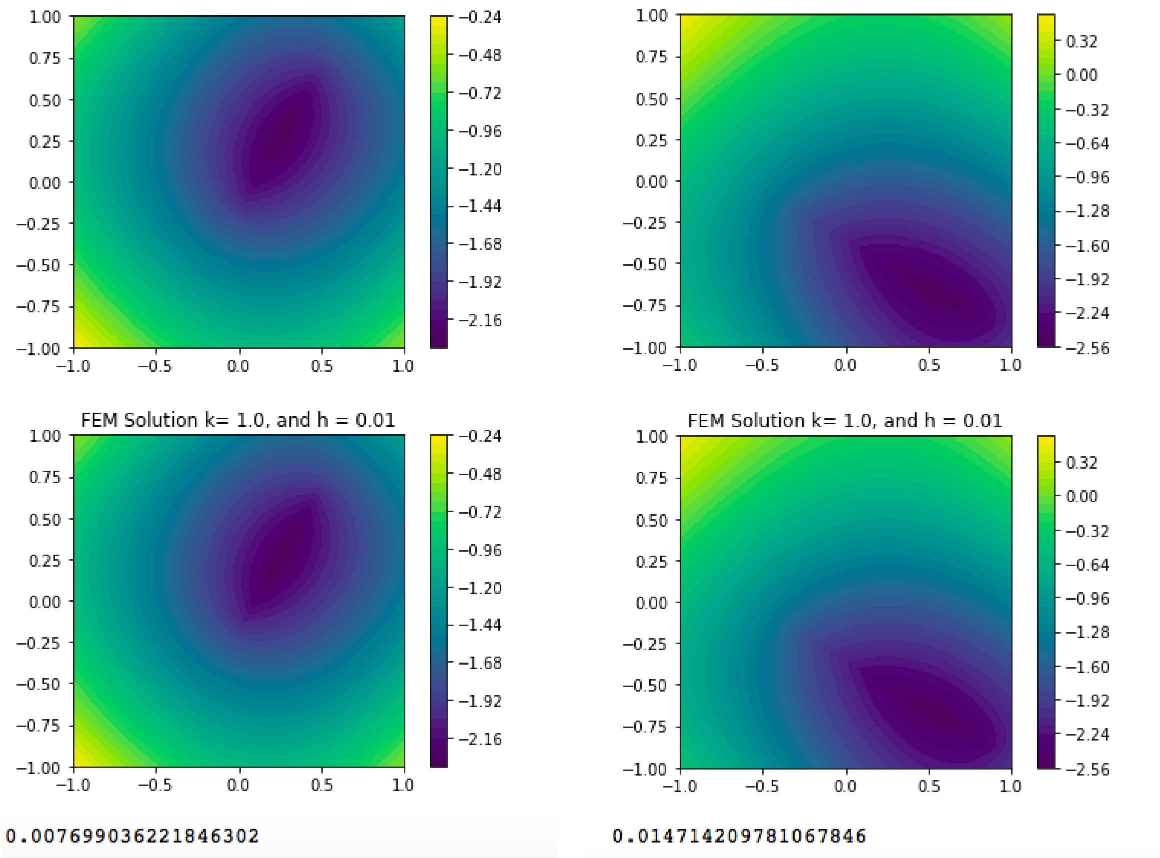

FIGURE 1. Top: Solutions computed for two different slit locations from dimensionally reduced approximation (34), $h = 0.01$. Bottom: FEM solutions for corresponding full problem (1). The numerical figure in each column is the computed maximum error between the two.

then we have

$$\|u_h - u_0\|_{L^\infty(\Omega)} \leq Ch_{max}.$$

We remark that when the line segments S_0^j intersect at points, for finite h the strips S_h^j overlap for areas of $O(h^2)$, which will not affect the limit of the Lippman-Schwinger formulation. If the segments were to overlap for nontrivial portions of the line, the Lippman-Schwinger formulation and its limiting problem (28) would double count these portions, which would correspond to a different coefficient n_h^2. For such a medium, the line segments should just be redefined so as not to overlap.

5. Numerical simulations for the forward problem

In this section we investigate the accuracy of the limiting solution u_0 given in general by (28). For the solutions of these limiting integral equations, we use a one-dimensional collocation method with piecewise linear basis functions and the FEniCS assemble function to compute the integrals which form the system matrix. These one-dimensional solutions are inserted into the right hand side of (30) to obtain the approximate solution on all of Ω. For the brute force solution to (27) we use FEniCS to compute a piecewise linear FEM solution directly.

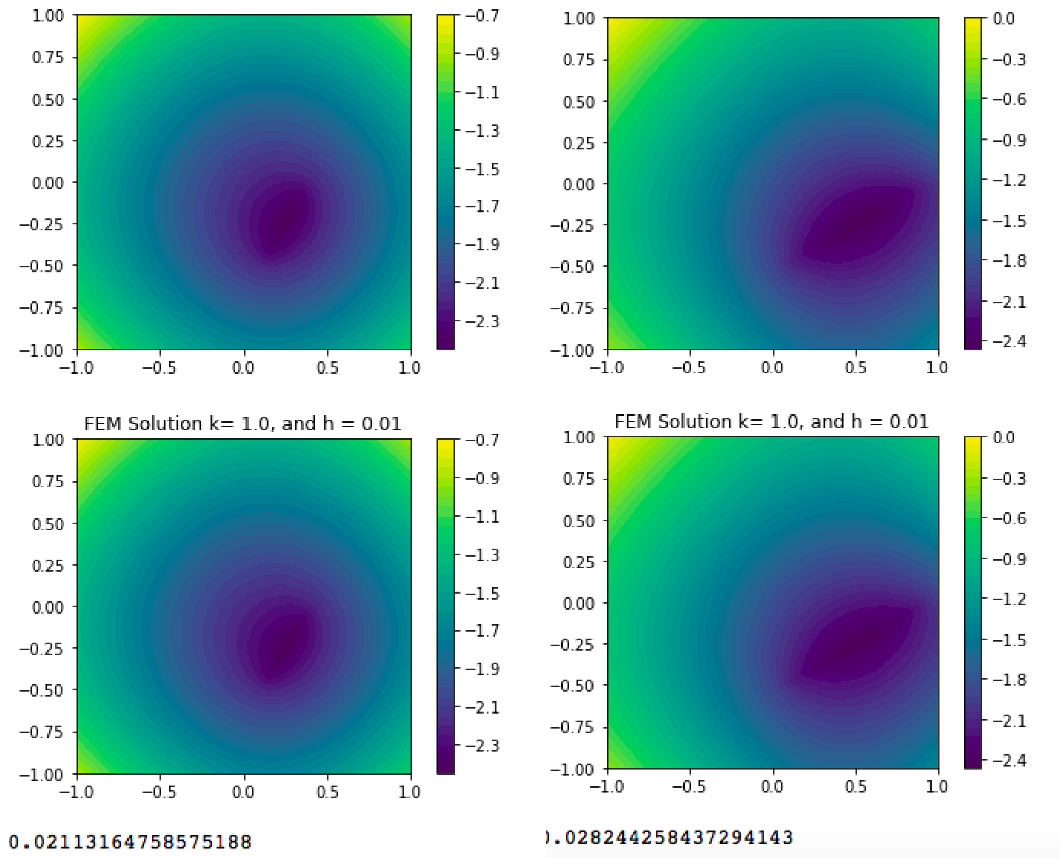

FIGURE 2. Top: Solutions computed for two more slit locations from dimensionally reduced approximation (34), $h = 0.01$. Bottom: FEM solutions for corresponding full problem (1). The numerical figure in each column is the computed maximum error between the two.

We first treat the case that the slit is at the origin, positioned horizontally, and of unit length. In this base case, the limiting one dimensional problem is to solve for $u_0(x_1)$ on the interval $[-1/2, 1/2]$,

$$u_0(x_1) = u_{\mathbf{i}}(x_1, 0) + k^2 \int_{-1/2}^{1/2} G((x_1, 0), (y_1, 0)) n_0(y_1) u_0(y_1) dy_1, \tag{31}$$

where $u_{\mathbf{i}}$ is the background solution and G is the Green's function for the larger two-dimensional domain. To solve this integral equation we use a straightforward collocation method and write the solution as

$$u_0(x_1) \approx \sum_{i=1}^{M} c_i \phi_i(x_1),$$

where M is the number of nodes and ϕ_i are piecewise linear basis functions, and we set (31) to hold for x_1 at all node points. For a general configuration of the slit, we define the affine coordinate transformation from original coordinates y_1 and y_2 to yield $\tilde{y}_1$ and $\tilde{y}_2$:

$$\begin{pmatrix} \tilde{y}_1 \\ \tilde{y}_2 \end{pmatrix} = a \begin{pmatrix} y_1 \\ y_2 \end{pmatrix} + b, \tag{32}$$

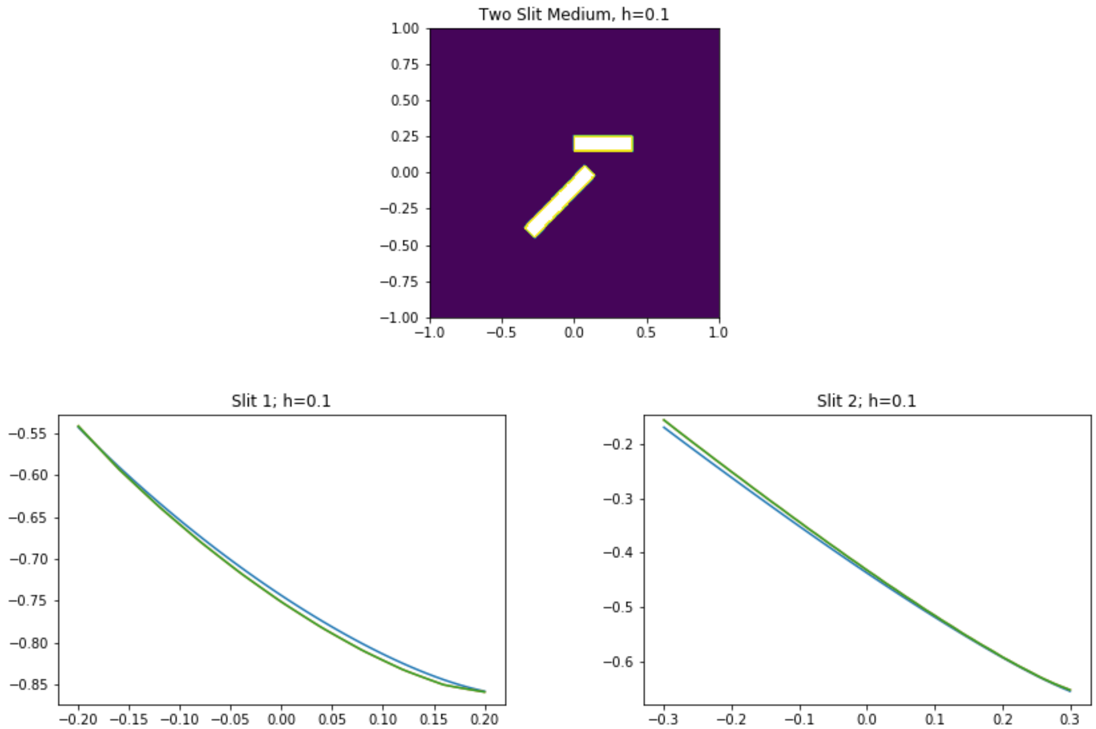

FIGURE 3. Comparison of solutions from the FEM solution to (27) (blue) and the $1-d$ collocation solution to (28) (green) on two slits for larger $h = 0.1$. Top: Slit geometry. Bottom left: Solutions on flat slit. Bottom right: Solutions on angled slit.

where

$$a = \frac{1}{l}\begin{pmatrix}\cos\theta & -\sin\theta \\ \sin\theta & \cos\theta\end{pmatrix}$$

is the rotation matrix with scaling corresponding to slit length l, and

$$b = -a\begin{pmatrix} q_1 \\ q_2, \end{pmatrix}$$

where (q_1, q_2) is the center of the slit. We use the inverse affine transformation

$$\begin{pmatrix} y_1 \\ y_2 \end{pmatrix} = a^{-1}\left[\begin{pmatrix} \tilde{y}_1 \\ \tilde{y}_2 \end{pmatrix} - b\right] \tag{33}$$

in equation (4) to calculate the full solution and also the asymptotic approximation. Let $\tilde{u}(\tilde{x}) = u(x)$ and use similar notation for all of the other functions in transformed coordinates to obtain

$$\tilde{u}(\tilde{x}) - \tilde{u}_{\mathbf{i}}(\tilde{x}) = \frac{1}{\det a}\int_{-h/2}^{h/2}\int_{-1/2}^{-1/2} G(x(\tilde{x}_1, \tilde{x}_1), y(\tilde{y}_1, \tilde{y}_2))\left(\frac{\tilde{n}_0}{h} - 1\right)\tilde{u}(\tilde{y}_1)d\tilde{y}_1 d\tilde{y}_2.$$

As the parameter h approaches zero, the integral can likewise be reduced to the one-dimensional equation

$$\tilde{u}_0(\tilde{x}_1) - \tilde{u}_{\mathbf{i}}(\tilde{x}_1, 0) = \frac{1}{\det a}\int_{-1/2}^{1/2} G\left(a^{-1}\left(\begin{pmatrix}\tilde{x}_1 \\ 0\end{pmatrix} - b\right), a^{-1}\left(\begin{pmatrix}\tilde{y}_1 \\ 0\end{pmatrix} - b\right)\right)\tilde{n}_0\tilde{u}_0 d\tilde{y}_1,$$

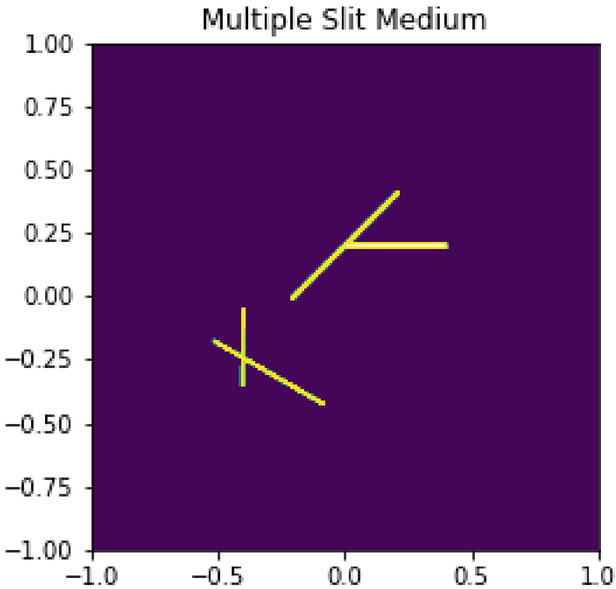

FIGURE 4. Medium with four slits, touching and crossing. Here $h = 0.01$ and $n_0 = 1$ in all four slits.

which we also solve by collocation. Once u_0 is found, to compute $u(x)$ for any $x \in \Omega$ we can use the formula

$$u(x) - u_{\mathbf{i}}(x) \approx \frac{1}{\det a} \int_{-1/2}^{1/2} G\left(x, a^{-1}\begin{pmatrix} \tilde{y}_1 \\ 0 \end{pmatrix} - a^{-1}b\right) \tilde{n}_0 \tilde{u}_0 d\tilde{y}_1. \tag{34}$$

This is similar to (9) in the reference case, and involves the computation of one-dimensional integrals only.

In Figure 1 and Figure 2 we compare surface plots on all of Ω for forward solutions computed from (34) and the FEM solution to the original PDE (27) for four different slit locations, angles, and lengths and small $h = 0.01$, with a contrast of $100:1$ and $k = 1$. In all four cases there is only one slit. The maximum error between the two is quite small in all cases.

In the next experiment, shown in Figure 3, we consider a medium with two slits, and use a larger $h_1, h_2 = 0.1$. The contrast in this case is $10:1$ on both slits and $k = 1$. We compare the limiting one-dimensional solutions with the restrictions of the the FEM solutions to the center lines S_0^1, S_0^2 of the inhomogeneities. The solutions continue to be well approximated, although one sees a bit more error due to larger h.

Finally, in Figure 5, we consider the field when the medium has four slits which partially touch and cross, as shown in Figure 4. Here $k = 1$, $n_0^{(j)} = 1$, and $h_j = 0.01$ for $j = 1, \ldots, 4$. In the figure we can see the comparisons to the restrictions of the FEM solutions, and note again that the interactions of the inhomogeneities are well captured.

6. The high contrast inverse problem

The asymptotic approximation shown above provides a lower-dimensional and therefore computationally inexpensive forward solver for the field in the presence of a thin high contrast inhomogeneity. If one knows *a priori* that the medium contains a certain number (or even a maximum

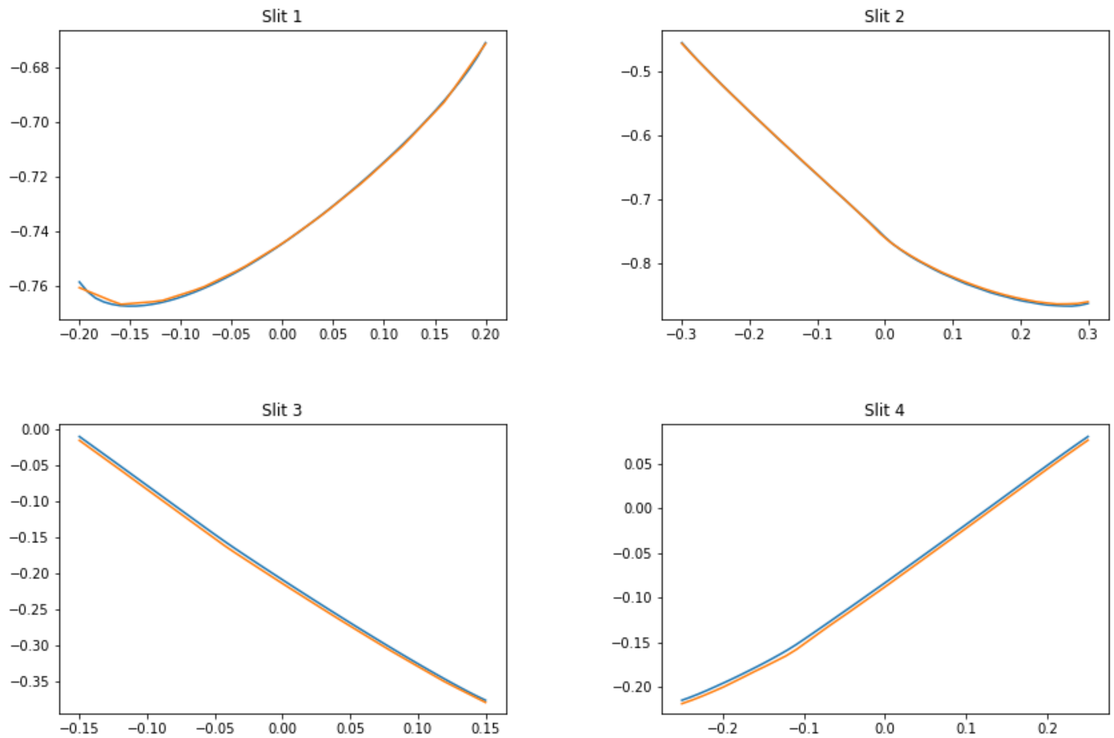

FIGURE 5. Comparison of solutions from the FEM solution to (27) (blue) and the $1-d$ collocation solution to (28) (orange) on multiple slits from Figure 4. Top left: Horizontal slit. Top right: Angled slit touching the horizontal. Bottom left: Vertical slit. Bottom right: Angled slit crossing the vertical.

number) of inhomogeneities of this form, such a solver can be used in conjunction with optimization to recover them.

We assume here that $\Omega = (-1,1) \times (-1,1) \in \mathbb{R}^2$, $n_0 \equiv 1$, $k = 1$. To start we assume we have only one slit with which is transformed by some unknown scaling, rotation, and translation. We do not assume we know h. For synthetic data, we will solve the full equation (27) with FEniCS FEM solutions as in the last section and read u on $\partial\Omega$ for 4 piecewise constant Neumann sources. We then use the BFGS optimization routine in SciPy to image the slit, that is we optimize over the angle, length, and center point of the slit in the formula (34). We minimize

$$F(a,b) = \int_{\partial\Omega} |V(x;a,b) - f(x)|^2 ds, \tag{35}$$

where $V(x;a,b)$ are the solutions computed on the boundaries using the dimensionally reduced (34) for the four sources, and f is our synthetic data. Note that we do not use nor do we assume we know h in the inversion procedure, but our plots of the resulting slits are thickened by h for illustration purposes. We do not recover h, either; to do that one would need a correction term, which will be the subject of future work. In Figures 6, 7, 8, 9, and 10 we demonstrate results of the optimization procedure. In all cases we successfully find the location, angle and length of the slit.

In the final example we attempt to recover two slits, while still using only four sources. In Figure 11 we initialize with two horizontal slits at the center and on top of each other. The algorithm

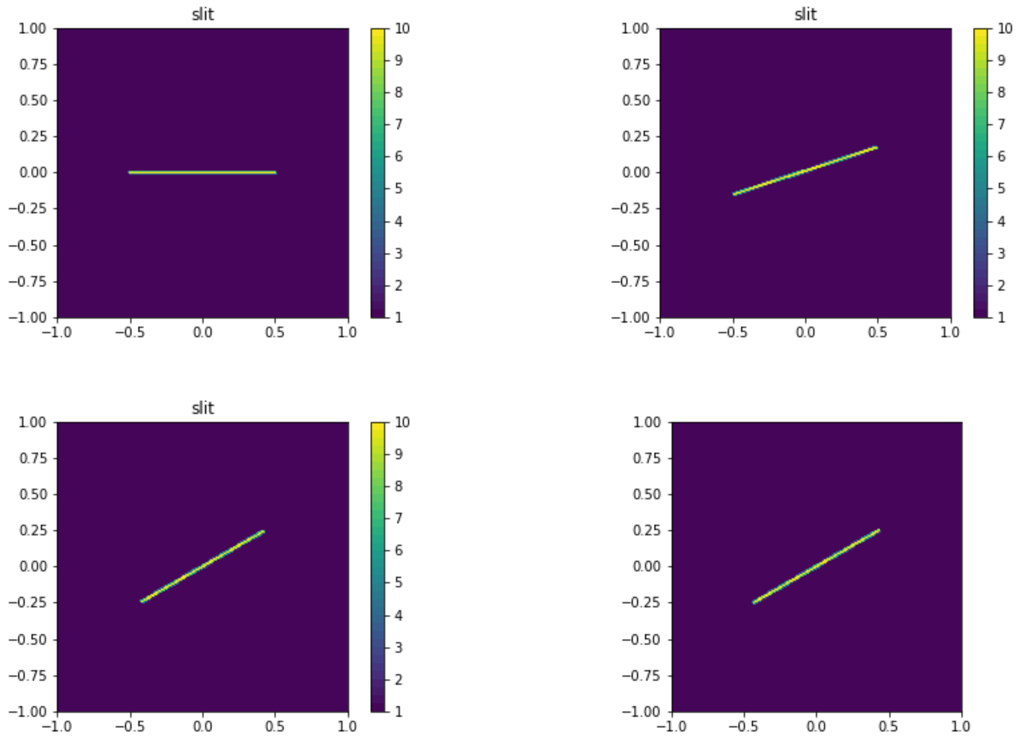

FIGURE 6. Recovery experiment, $h = 0.01$. Top left: initial guess. Top right: intermediate iteration. Bottom left: final iteration. Bottom right: actual slit.

separates them and finds their locations and angles successfully. We note that we expect the recovery of more complicated geometries and several slits will require more sources. This is the subject of future work.

7. Remarks on extensions to Maxwell

Consider the time harmonic Maxwell equation with a thin scatterer present and $\mu = 1$,

$$\nabla \times \nabla \times E - k^2 n^2 E = 0 \quad \text{on } \mathbb{R}^3, \tag{36}$$

where the vector valued E is the electric field, $k > 0$ is the normalized temporal frequency, and n^2 denotes the squared index of refraction,

$$n^2(\overline{x}, x_3) = \begin{cases} 1, & |x_3| > h/2, \\ n_0(\overline{x})/h, & |x_3| < h/2, \overline{x} \in S_0, \\ 1, & |x_3| < h/2, \overline{x} \notin S_0, \end{cases} \tag{37}$$

taking Silver-Muller radiation conditions at infinity. From a somewhat more difficult analysis than for Helmholtz, one finds the limiting (two dimensional) system [3], [2]

$$\begin{aligned} E_1^{(0)}(\overline{x}) &= (E_{\mathbf{i}})_1(\overline{x}, 0) + k^2 \int_{S_0} \mathcal{G}(\overline{x}, 0, \overline{x}', 0) n_0 E_1^{(0)}(\overline{x}') d\overline{x}', \\ E_2^{(0)}(\overline{x}) &= (E_{\mathbf{i}})_2(\overline{x}, 0) + k^2 \int_{S_0} \mathcal{G}(\overline{x}, 0, \overline{x}', 0) n_0 E_2^{(0)}(\overline{x}') d\overline{x}', \\ E_3^{(0)}(\overline{x}) &= 0, \end{aligned} \tag{38}$$

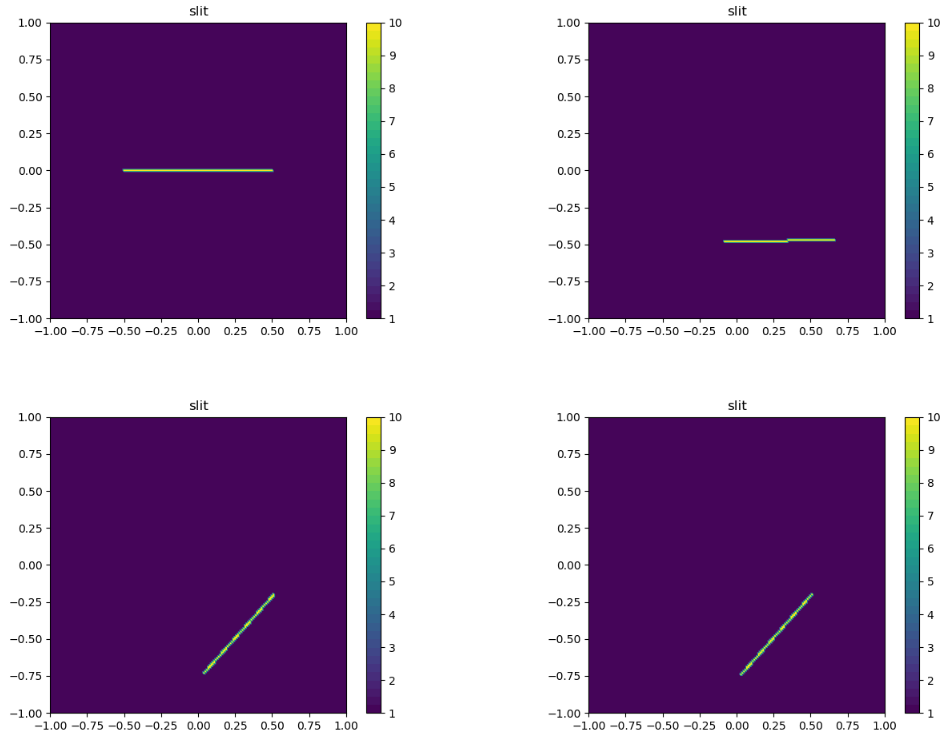

FIGURE 7. Recovery experiment, $h = 0.01$. Top left: initial guess. Top right: intermediate iteration. Bottom left: final iteration. Bottom right: actual slit.

for $\overline{x} \in S_0$, and $\mathcal{G}$ the Helmholtz free space fundamental solution. In [1], a direct inversion method was proposed for this problem which made use of the next-order asymptotics. However, a more robust approach should result from inserting the two-dimensional approximation (38) into the formulation for Maxwell's equations of Lippman-Schwinger type which was analyzed in [7]. Since the measurements are on the boundary (which is assumed to be bounded away from the scatterer), there will be no singularity in the integral even in limiting case. This will yield an approximation to the scattered field on the boundary which involves only two-dimensional integrals an hence an efficient forward solver to do optimization as above. Indeed since for x in the far field we have

$$E_h(x) = E_{\mathbf{i}}(x) + k^2 \int_{S_h} \mathcal{G}(x, x') \left(n_0(\overline{x}')/h - 1 \right) E_h(x') dx' + \int_{S_h} \nabla_x^2 (\mathcal{G}(x, x')) \left(n_0(\overline{x}')/h - 1 \right) E_h(x') dx', \tag{39}$$

we take the limit in the same way to find

$$E_h(x) \approx E_{\mathbf{i}}(x) + k^2 \int_{S_0} \mathcal{G}((x, (\overline{x}', 0)) n_0(\overline{x}') E^{(0)}(\overline{x}') d\overline{x}' + \int_{S_0} \nabla_x^2 (\mathcal{G}(x, (\overline{x}', 0))) n_0(\overline{x}') E^{(0)}(\overline{x}') d\overline{x}'. \tag{40}$$

Note that for x in the far field, or on the boundary for bounded domains, the integrals are nonsingular. Furthermore, the first-order term, which is again only two dimensional in complexity, can be incorporated to improve the approximation.

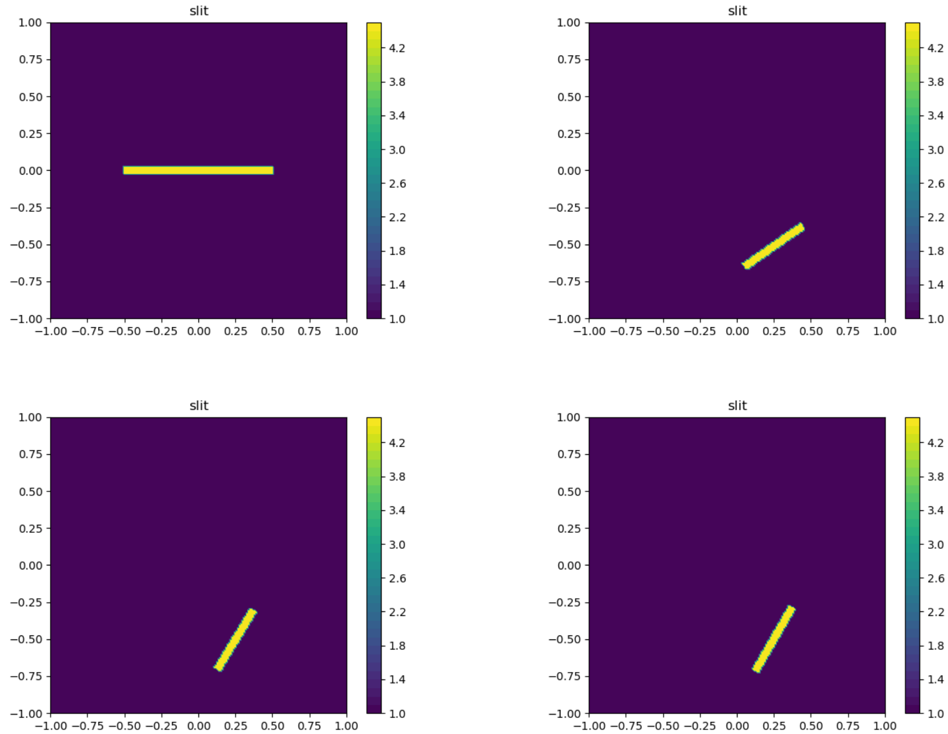

Figure 8. Recovery experiment, $h = 0.05$. Top left: initial guess. Top right: intermediate iteration. Bottom left: final iteration. Bottom right: actual slit.

Acknowledgments

The research of Shari Moskow is supported in part by NSF grant DMS-1715425. The research of David M. Ambrose is supported in part by NSF grant DMS-1515849. The research of Gideon Simpson is supported in part by NSF grant DMS-1818716. Drexel undergraduate students Eesha Das Gupta and Valentina Ozornina were partially supported by an REU supplement to DMS-1715425.

References

[1] D.M. Ambrose, J. Gopalakrishnan, S. Moskow, and S. Rome. Scattering of electromagnetic waves by thin high contrast dielectrics ii: asymptotics of the electric field and a method for inversion. *Commun. Math. Sci.*, 15(4):1041–1053, 2017.

[2] D.M. Ambrose and S. Moskow. Scattering of electromagnetic waves by thin high contrast dielectrics: effects of the object boundary. *Commun. Math. Sci.*, 11(1):293–314, 2013.

[3] H. Ammari, H. Kang, and F. Santosa. Scattering of electromagnetic waves by thin dielectric planar structures. *SIAM J. Math. Anal.*, 38(4):1329–1342, 2006.

[4] Liliana Borcea. Asymptotic analysis of quasi-static transport in high contrast conductive media. *SIAM J. Appl. Math.*, 59(2):597–635, 1999.

[5] Liliana Borcea and George C. Papanicolaou. Network approximation for transport properties of high contrast materials. *SIAM J. Appl. Math.*, 58(2):501–539, 1998.

[6] D. Colton and R. Kress. *Inverse Acoustic and Electromagnetic Scattering Theory*, volume 93 of *Applied Mathematical Sciences*. Springer.

[7] A. Kirsch and A. Lechleiter. The operator equations of Lippmann-Schwinger type for acoustic and electromagnetic scattering problems in L^2. *Appl. Anal.*, 88(6):807–830, 2009.

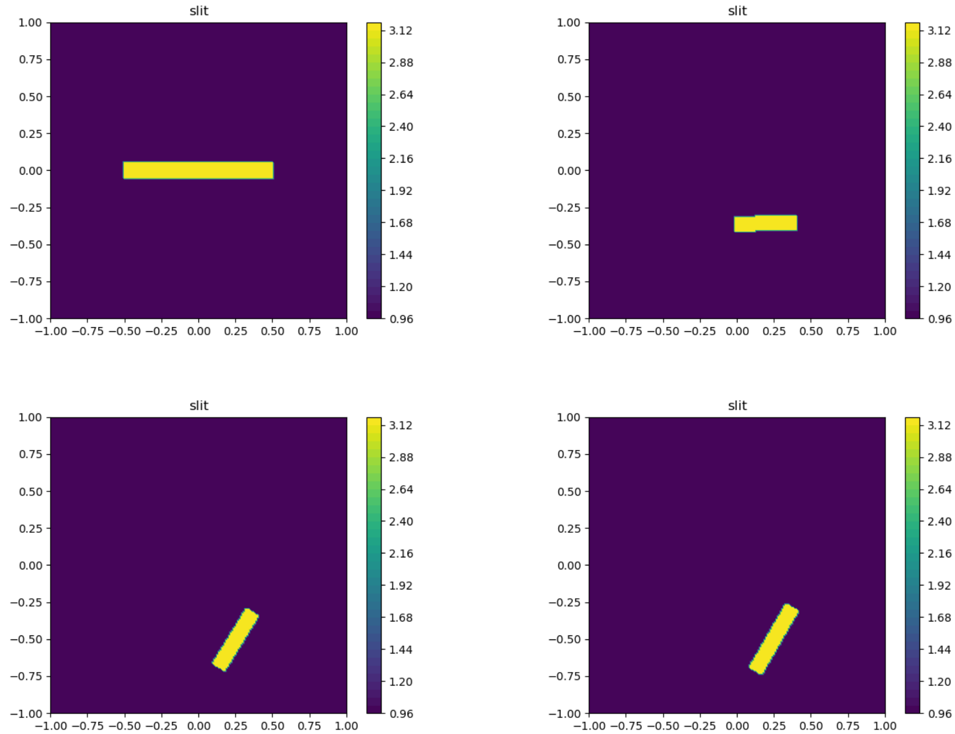

Figure 9. Recovery experiment, $h = 0.1$. Top left: initial guess. Top right: intermediate iteration. Bottom left: final iteration. Bottom right: actual slit.

[8] S. Moskow, F. Santosa, and J. Zhang. An approximate method for scattering by thin structures. *SIAM J. Appl. Math.*, 66(1):187–205 (electronic), 2005.

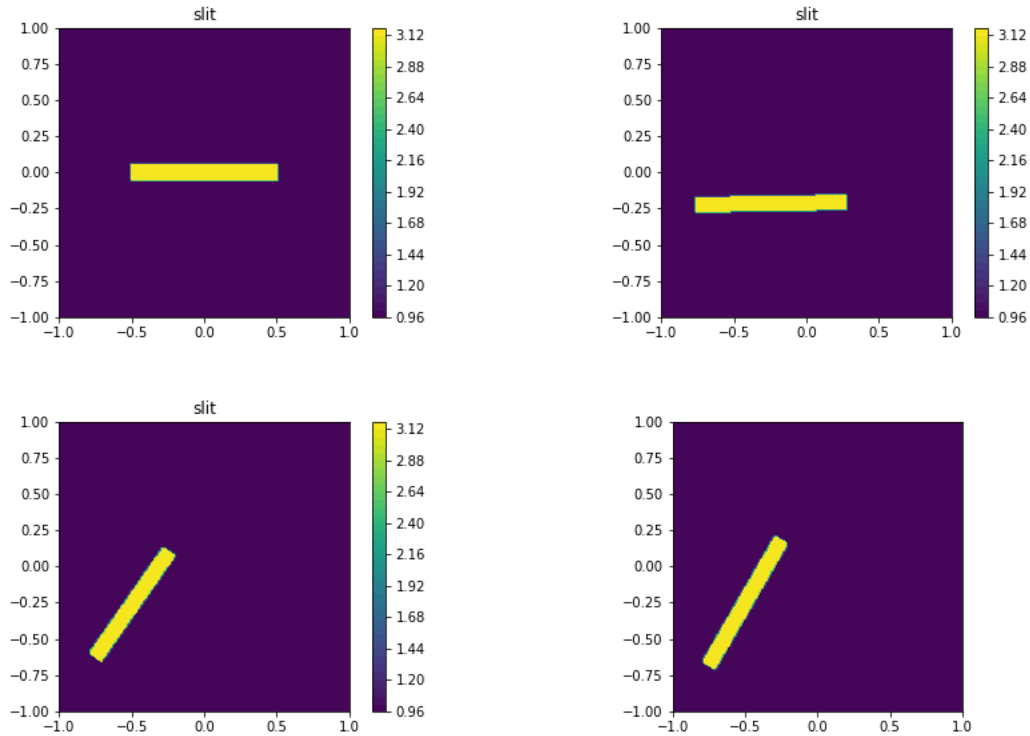

FIGURE 10. Recovery experiment, $h = 0.1$. Top left: initial guess. Top right: intermediate iteration. Bottom left: final iteration. Bottom right: actual slit.

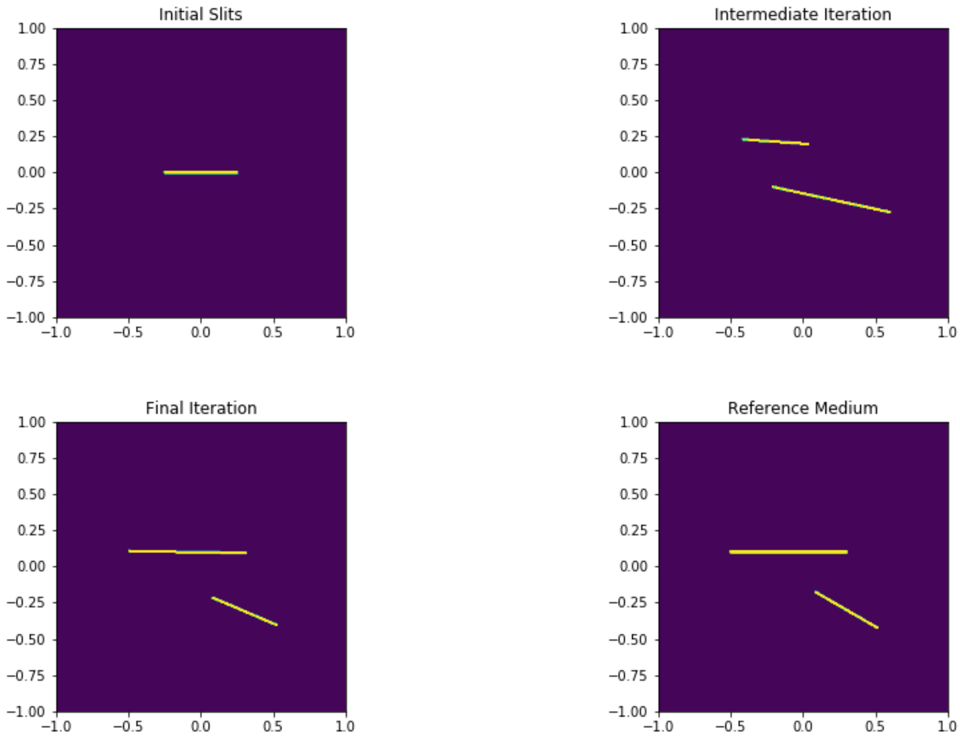

FIGURE 11. Recovery experiment, $h = 0.01$. Top left: initial guesses of two slits on top of each other. Top right: intermediate iteration. Bottom left: final iteration. Bottom right: actual reference medium slits.